Answers in Depth, Vol. 4, (2009), September 9, 2009.
https://assets.answersingenesis.org/doc/articles/aid/v4/radiohalos-cooma-metamorphic-complex.pdf

Radiohalos in the Cooma Metamorphic Complex, New South Wales, Australia: The Mode and Rate of Regional Metamorphism

Andrew A. Snelling, Ph.D., Answers in Genesis

This paper was originally published in the *Proceedings of the Sixth International Conference on Creationism*, pp.371–387 (2008) and is reproduced here with the permission of the Creation Science Fellowship of Pittsburgh (www.csfpittsburgh.org) and the Institute for Creation Research, Dallas.

Abstract

The Cooma metamorphic complex in southeastern Australia is a classical example of regional metamorphic zones centered on a granodiorite generated by partial melting at the highest metamorphic grade. Samples collected along a traverse from the low-grade biotite and then andalusite zone schists through the high-grade K-feldspar and migmatite zone gneisses into the central granodiorite contain increasing numbers of Po radiohalos with increasing metamorphic grade. The highest Po radiohalo numbers are in the high-grade zones and the granodiorite. These radiohalo patterns correlate with the Po radiohalos being generated by the hydrothermal fluids flowing out of the central granodiorite as it crystallized and cooled, their numbers diminishing as the hydrothermal fluid flow decreased outwards. This is further evidence consistent with the hydrothermal transport model for Po radiohalo formation. Furthermore, generation of the regional metamorphic complex only required 12–20 days, based on the catastrophic granite formation of the adjacent Murrumbidgee Batholith whose heat and hydrothermal fluids generated the regional metamorphic zones of the complex from the mineral constituents of the original fossiliferous sediment layers, then the central granodiorite as a consequence. This sequence of outcomes is consistent with creationist models for catastrophic granite formation and regional metamorphism driven by catastrophic plate tectonics during the year-long biblical Flood.

Keywords

regional metamorphism, Cooma, southeastern Australia, Po radiohalos, ^{238}U radiohalos, granodiorite, metamorphic zones, hydrothermal fluids, catastrophic granite generation, creationist model for regional metamorphism

Introduction

The Cooma granodiorite was first mapped by Browne[1] and is a small, elliptical pluton centered approximately on the township of Cooma in southern New South Wales, 300 km south-southwest of Sydney (fig. 1 inset). The pluton is about 8 km in maximum dimension and has a surface exposure of 14–20 km^2, depending on where its gradational contact with the surrounding migmatites is placed.[2] When mapped, the pluton was found to be central to a sequence of roughly concentric prograde regional metamorphic zones.[3–5] In fact, the Cooma metamorphic complex is considered to be a classic geological area for regional metamorphic zones, because it is one of the first localities where andalusite-sillimanite type regional metamorphism was described.[6, 7] Furthermore, the Cooma granodiorite itself is also regarded as a classic geological example of a pluton produced by a low degree of partial melting of the metasediments at the heart of a regional metamorphic complex (fig. 1).[8]

The Cooma metamorphic complex has a mapped outcrop area exceeding 300 km^2, and probably extends over a similar area beneath the local cover of Tertiary basalt. Isograds can be traced over 30 km northwards adjacent to the Murrumbidgee Batholith.[9] Based mainly on the work of Joplin[10,11] and Hopwood,[12, 13] Chappell and White[14] recognized a series of metamorphic zones delineated by the appearance of chlorite, biotite, andalusite, sillimanite, and granitic veining, respectively. Approximate equivalents are chlorite zone–greenschist facies; biotite and andalusite zones–amphibolite facies; sillimanite and migmatite zones–granulite facies.[15] Some additional metamorphic zones have been distinguished by subdividing the andalusite and sillimanite zones on the basis of the first appearances of cordierite, andalusite and K-feldspar.[16] The zoning is markedly asymmetric. The belt of highest grade rocks and the enclosed Cooma granodiorite are located towards the eastern margin of the complex (fig. 1), with the regional aureole extending approximately 3 km to the east, but nearly 10 km to the west. At least four,[17] and possibly seven,[18] separate deformation fabrics can be distinguished in the metasediments of the Cooma complex. The exception is the Cooma granodiorite, which preserves only the last foliation, suggesting that it was emplaced late in the development of the complex.[19, 20]

Cooma Metamorphic Complex

The stratigraphic sequence that transitions into the higher grade zones of the Cooma metamorphic complex has been estimated at approximately 3,000 meters thick, as measured from beyond the western edge of the low grade zones eastward into the complex.[21, 22] Four units have been mapped, none of which are completely free of low grade metamorphic effects. The lowest unit, to the east stratigraphically above the high grade zone rocks of the central complex, is a sequence of regularly bedded sandstones and shales. The sandstones are thinly bedded, averaging 10–45 cm thick, and the shaly units are often characterized by finely laminated alternating units of grey shale and white sandy shale. About halfway up this unit 1, which is at least 915 m thick, is an 18 m thick massive sandstone bed. Otherwise, gradually towards the top of this formation massive clayey shales and lenses of black shales appear. The overlying unit 2 is a sequence of massive thickly bedded sandstones, averaging 2.5–3.5 m thickness per bed, and often separated by thin layers of sandy shale. These shale layers appear regularly throughout the sequence, but together make up no more than one fifth of the total 425 m thickness of unit 2. Above this is unit 3, a 950 m thick sequence of green and grey shales, with occasional lenticular black shales and very thinly laminated siliceous bands. At the base of the unit is a massive black shale layer, over which lies a fine-grained grey siltstone, while towards the top, the monotonous sequence of shales is broken by a thin quartz-rich sandstone layer. The top of the unit 3 shale succession then grades by interlayering into the volcanic sequence of unit 4, which is at least 455 m thick. At the base are a few small limestone lenses, and clay shales. The volcanics, now greenschists, are strongly foliated, and porphyritic in quartz. They probably were originally trachytic or andesitic lava flows and their detrital equivalents.

The top of this unit 4 volcanic sequence is not exposed. Abundant fossilized graptolites have been recorded still preserved in the shale layers within these lowest grade zone rocks, approximately 8 km west of the Cooma granodiorite, in the outer area of the metamorphic complex.[23] Biostratigraphically these graptolites equate to upper Ordovician fossil zones elsewhere in the Lachlan Fold Belt of New South Wales.[24, 25] Thus the volcanics at the top of this strata sequence could be lower Silurian. Otherwise, the other units are typical of other upper Ordovician turbidite strata sequences of shales and subgreywacke sandstones found elsewhere in the Lachlan Fold Belt. Furthermore, detrital zircon and monazite grains with inherited U-Pb ages have been found in both these metamorphosed sediments of the Cooma metamorphic complex, at least as far out as the low grade biotite zone, and in the Cooma granodiorite which was derived from those sediments by partial melting.[26] The U-Pb ages of these detrital zircon grains ranged from 450 Ma to 3538 Ma, with 50% of the grains in the 450–600 Ma range and 30% in the 800–1250 Ma range. The detritral monazite grains yielded similar U-Pb ages, with most grains in the 410–650 Ma range. Similar detrital zircon grains are also found in graptolite fossil-bearing upper Ordovician turbidite sediments elsewhere in the Lachlan Fold Belt.[27] The U-Pb ages of those zircon grains were similarly in the ranges of 480–630 Ma (60% of grains in one sample) and of 470–600 Ma (50% of grains in a second sample), with 20% and 25% of grains (respectively) yielding 1000–1300 Ma ages.

The metamorphism in the Cooma complex (fig. 1) is classified as low-P, high-T (LPHT),[28, 29] the metamorphic assemblages resembling those in the Abukuma andalusite-sillimanite metamorphic belt of Japan:[30]

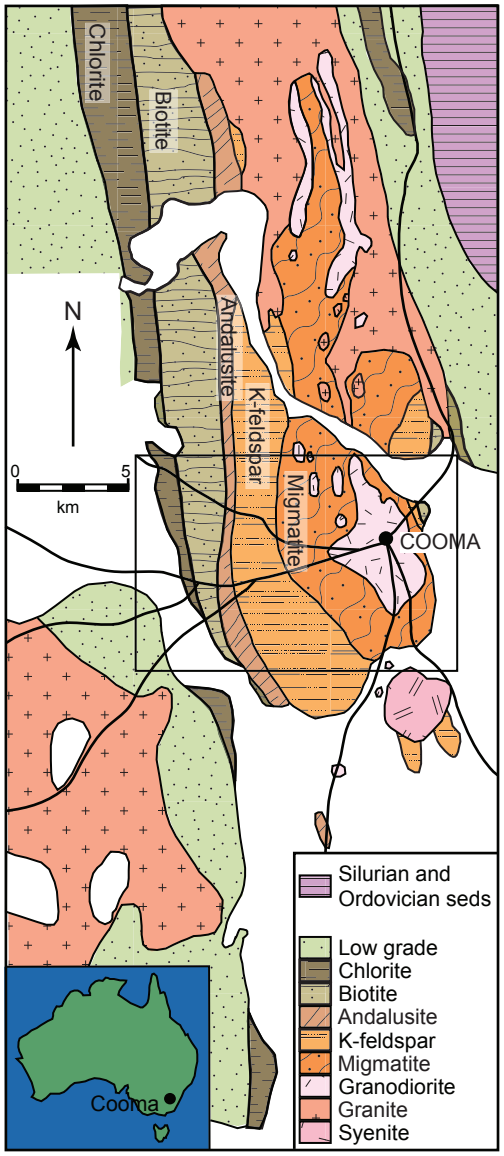

Fig. 1. The Cooma metamorphic complex, southeastern Australia, showing the zones of regional metamorphism of increasing grade surrounding a central granodiorite, coinciding with the town of Cooma. The marked area is enlarged in Fig. 2.

Chlorite zone

The metapelites are characterized by the mineral assemblage

chlorite+muscovite+quartz, with minor albite, calcite, and opaque (iron oxide) minerals.[31–33] Muscovite is generally far more abundant than chlorite, and both minerals occur as highly elongate grains rarely longer than 0.1 mm. The metapsammites contain the same minerals, with local detrital K-feldspar grains sometimes partly altered to muscovite, whereas former detrital biotite and plagioclase grains have been altered to chlorite and albite respectively.

Biotite zone

This zone is differentiated from the chlorite zone by the first appearance of biotite in metapelites, resulting in the characteristic mineral assemblage quartz+albite+biotite+muscovite±chlorite, with minor tourmaline and opaque (iron oxide) minerals. The first biotite to appear is green and weakly pleochroic, but this variety gives way to a more strongly pleochroic brown biotite further into the zone.[34] Grain sizes differ little from those in the chlorite zone, except the mica grains range up to 0.2 mm in length, and biotite porphyroblasts can be as long as 0.7 mm.[35]

Andalusite zone

This zone is defined on the presence of andalusite alone, without accompanying sillimanite. Its characteristic mineral assemblage is andalusite+cordierite+biotite+muscovite+quartz+albite, with minor tourmaline, opaque (iron oxide) minerals and zircon. Andalusite porphyroblasts range widely in size from approximately 0.5 to 5.0 mm in their longest dimension. Johnson, Vernon, and Hobbs[36] inserted an extra zone between the biotite and andalusite zones, basing its identification on the first appearance of cordierite. Named the cordierite zone, it has the same mineral assemblage as the andalusite zone, but minus andalusite, whereas cordierite is still present in the andalusite zone. In this cordierite zone the cordierite porphyroblasts range from 1.0 to 10.0 mm in longest dimension, but are extensively replaced by retrogressive aggregates of sericite, biotite and chlorite. On the other hand, in the andalusite zone some andalusite is intimately related with replaced cordierite porphyroblasts.

K-feldspar zone

This zone is defined by the first appearance of metamorphic K-feldspar (orthoclase), which marks the onset of grain coarsening into a gneissic texture. The characteristic mineral assemblage is K-feldspar + cordierite + andalusite + biotite + plagioclase + quartz ± sillimanite, with minor tourmaline, zircon and opaque (iron oxide) minerals. Muscovite is commonly present as relatively large grains, which appear though to be of retrograde origin.

Migmatite zone

This zone is vaguely defined by the presence of abundant granitic "veins" in a sillimanite-andalusite-biotite gneiss. The "veins" consist chiefly of quartz, K-feldspar and lesser plagioclase, and vary in thickness from a few millimeters to a few centimeters. Overall, the metasedimentary rocks of this zone are commonly divided into mottled metapelitic gneisses and banded metapsammitic gneisses.[37, 38] The mottling in the metapelitic gneisses is due to intergrowths of green-brown biotite, quartz and andalusite pseudomorphing cordierite porphyroblasts. The banded metapsammitic gneisses are composed of a dark/light compositional layering. These metapelitic and metapsammitic migmatites are found all the way around the granodiorite in gradational contact with it. The more pelitic rocks have leucosomes of granitic material surrounded by coarse-grained mesosomes. The leucosomes are composed of quartz, K-feldspar and plagioclase, and range in width from 2 mm to 5 cm. Some leucosomes have distinct biotite-rich selvedges and may contain fresh cordierite crystals up to 5 mm across.[39]

Major and trace element abundances suggest that the high-grade metapelitic and metapsammitic gneisses of the migmatite and K-feldspar zones surrounding the granodiorite are the geochemical equivalents of the more distant, low-grade pelitic and psammitic schists.[40] However, the minor variation in the orthoclase-albite-anorthite ratio between the low-grade schists and high-grade gneisses would suggest otherwise.[41] Nevertheless, for the purpose of this study it was noted as significant that biotite is always present throughout the metamorphic complex from the biotite zone inwards through the migmatite zone into the granodiorite, while accessory zircons are similarly distributed.[42, 43] Williams also reported ^{238}U and ^{232}Th radiohalos surrounding tiny zircon and monazite grains respectively within biotite flakes from the K-feldspar and migmatite zones, as well as in the granodiorite, the latter confirmed by Snelling and Armitage,[44] along with abundant Po radiohalos. Furthermore, Snelling[45, 46] had reported finding Po radiohalos in metamorphic rocks, including through the zones within a regionally metamorphosed sequence of sandstone.[47] Thus, because Snelling[48] had proposed a model for regional

metamorphism involving hydrothermal fluids, and the hydrothermal fluid transport model for the formation of Po radiohalos involves the required Po isotopes being sourced from zircons in biotites,[49, 50] it was predicted that Po radiohalos would be found in all the biotite bearing schists and gneisses of the Cooma metamorphic complex.

Cooma granodiorite

The Cooma granodiorite contains the same minerals as the gneisses and migmatites, and lies within the cordierite-andalusite-K-feldspar zone. It is extremely quartz-rich (50%), and contains plagioclase, K-feldspar and biotite, with andalusite, sillimanite, cordierite and muscovite, some or all of the latter appearing to be secondary.[51–53] The biotite is crowded with ^{238}U and ^{232}Th radiohalos around inclusions of zircon and monazite respectively,[54] while Snelling and Armitage[55] have reported Po radiohalos are also prevalent. The granodiorite contains abundant xenoliths of the surrounding migmatites and, less commonly, the high-grade gneisses, quartz veins and pegmatites. This is consistent with the granodiorite having been derived by partial melting of a metasedimentary source, presumably the high-grade gneisses surrounding the granodiorite.[56] Thus the granodiorite has been classified as S-type[57] with normative corundum values of 5.82%,[58] indicating that it is strongly peraluminous. It is also very low in Na_2O and CaO, which has been attributed to its derivation from the surrounding metamorphosed Ca-poor Ordovician sediments.[59] This origin is supported by isotopic data.[60–64] The Cooma granodiorite is thus typical of "regional aureole" granites described by White, Chappell, and Cleary,[65] and Chappell and White.[66]

Radioisotopic data suggests that the Cooma granodiorite and the related metamorphic rocks thus cooled through the blocking temperature for most geochronological systems in the mid to late Silurian.[67] Pidgeon and Compston[68] obtained an Rb-Sr mineral isochron age for the granodiorite of 406±12Ma. The age of the high-grade gneisses was found to be similar to the granodiorite, but the low grade metasediments yielded a significantly older age of 450±11Ma (recalculated by Munksgaard[69]). Based on these results it was concluded that the granodiorite formed in situ by partial melting of the surrounding metasediments, the high-grade gneisses being associated with the emplacement of the granodiorite, whereas the higher ages in the low-grade metasediments perhaps indicated the original age of deposition, or the age of regional metamorphism pre-dating the high-grade metamorphism. Tetley[70] obtained a Rb-Sr whole-rock isochron age for the granodiorite of 410.0±19.0Ma, thus supporting the previously determined granodiorite age. However, Munksgaard obtained whole-rock Rb-Sr ages of 362±77Ma for the granodiorite, 375±55Ma for the high-grade gneisses, and 386±25Ma for the low-grade metasediments. He suggested these results implied the metasediments and the granodiorite were not fully equilibrated on a regional scale with respect to their Sr isotope composition at the time of metamorphism, and thus whole-rock samples would not give meaningful ages for the Cooma complex. Nevertheless, he showed that the Cooma granodiorite is similar in major- and trace-element composition to a calculated mixture of the surrounding schists and gneisses.

Preliminary results of ion-probe zircon U-Pb studies[71] yielded ages from zircon about 30Ma greater than the 410Ma age recorded by hornblende K-Ar and whole-rock Rb-Sr.[72] More detailed results have now been published.[73] Both monazite and zircon grains from the Cooma granodiorite and from the metasediments in each of the surrounding regional metamorphic zones were analyzed. Monazite in the migmatite and granodiorite were found to have recorded only metamorphism and granite genesis at 432.8±3.5Ma, whereas detrital zircon grains in the original sediments were unaffected by metamorphism until the inception of partial melting, when platelets of new zircon precipitated on the surfaces of the grains. These new growths of zircon crystals, although maximum in the leucosome of the migmatites, were best dated in the granodiorite at 435.2±6.3Ma. Thus the best combined estimate for the U-Pb age of the metamorphism and granite genesis is 433.4±3.1Ma. Because the detrital zircon U-Pb ages were found to have been preserved unmodified throughout metamorphism and magma genesis, Williams[74] concluded that this indicated the Cooma granodiorite was derived from lower Paleozoic source rocks with the same protolith as the Ordovician sediments found outcropping adjacent to the metamorphic complex in the same region. These U-Pb ages for the detrital zircon and monazite grains preserved in the metasediments and the granodiorite from the original Ordovician sediments were dominated by composite populations dated at 500–600Ma and 900–1200Ma, although almost 10% of the grains analyzed yielded apparent ages scattered from 1450Ma to 2839Ma, one grain even yielding an apparent age of 3538Ma.

The general consensus is that the Cooma granodiorite is an integral part of the regional metamorphic sequence, having formed by the in situ, or virtually in situ, partial melting of high-grade metasediments identical to those surrounding it.[75–84] However, Flood and Vernon[85] pointed out that an origin for the Cooma granodiorite from essentially in situ anatexis of the adjacent metasedimentary rocks was in apparent conflict

with the surrounding low-pressure metamorphic environment, unless unrealistically high and localized geothermal gradients were invoked. They suggested that subsequent to the granodiorite forming by partial melting of the adjacent high-grade migmatitic rocks, the granodiorite moved upwards as a diapiric intrusion, the high-grade envelope surrounding it having been dragged up to higher crustal levels with the intruding granitic diapir. Support for this model includes evidence for vertical movement along a transition zone between the andalusite zone schists and the K-feldspar zone gneisses (fig. 1), a step in metamorphic pressures at the sillimanite isograd, coinciding with the boundary between the gneisses and migmatites, and a steady pressure rise thereafter towards higher metamorphic grades.[86] All the metamorphism is regarded as part of the same relatively intact sequence, the thermal aureole having contracted towards the granodiorite during the later stages of the deformation associated with the regional metamorphism and the emplacement of the granodiorite.[87] Finally, Vernon, Richards, and Collins[88] have demonstrated that in situ partial melting of metapsammitic leucosome would have produced a magma of suitable composition to form the Cooma granodiorite, but this locally produced magma appears to have only contributed to the rising pluton of magma formed by deeper, more extensive accumulation of similarly derived magma, a model consistent with the U-Pb zircon data.[89]

Field Work

A field trip to the Cooma area was undertaken in late December, 2004. A west-east traverse was made through the metamorphic complex into the central granodiorite along major roads (fig. 2). Representative samples were collected from the biotite, andalusite, K-feldspar, and migmatite zones, as well as from the granodiorite, from outcrops in road cuts and on a small hill in Cooma itself. All nine sample locations are marked in Fig. 2. Views of some of the outcrops are shown in Fig. 3.

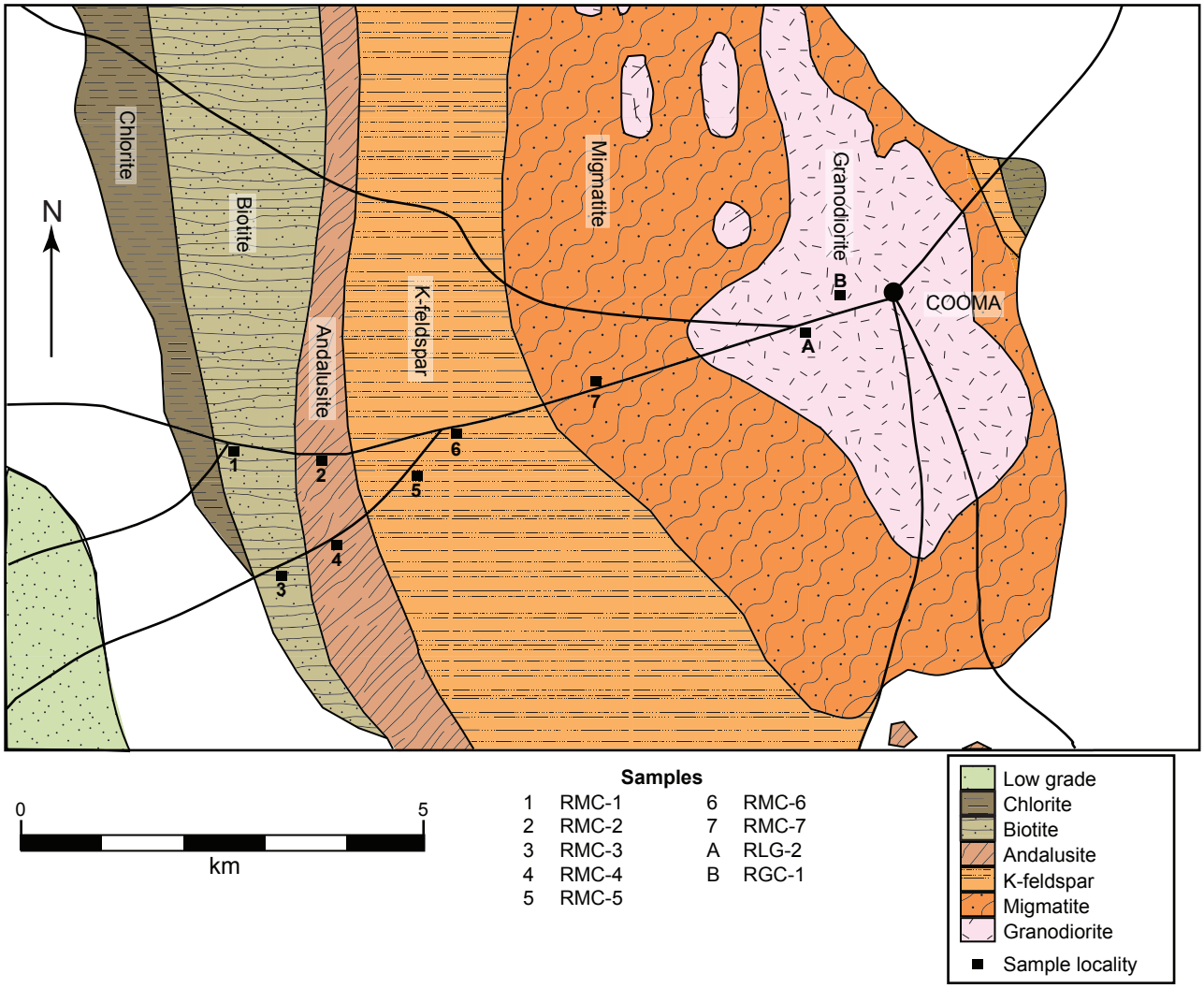

Fig. 2. Enlargement of the area marked in Fig. 1, showing an enlarged view of the regional metamorphic zones west of the Cooma granodiorite centered on the town of Cooma. The sample locations are shown along major roads.

Fig. 3. Typical views of the outcrops sampled (see fig. 2).
(a) Sample site RMC-3, a low-grade biotite zone schist.
(b) Sample site RMC-4, a low-grade andalusite zone schist
(c) Sample site RMC-7, high-grade migmatite zone gneiss
(d) Sample site RGC-1, the Cooma granodiorite on Nanny Goat Hill

Experimental Procedures

A standard petrographic thin section was obtained for each sample. In the laboratory, a scalpel and tweezers were used to pry flakes of biotite loose from the sample surfaces, or where necessary portions of the samples were crushed to liberate the constituent mineral grains. Biotite flakes were then hand-picked and placed on the adhesive surface of a piece of clear Scotch™ tape fixed to a bench surface with its adhesive side up. Once numerous biotite flakes had been mounted on the adhesive surface of this piece of clear Scotch™ tape, a fresh piece of clear Scotch™ tape was placed over them and firmly pressed along its length so as to ensure the two pieces of clear Scotch™ tape were stuck together with the biotite flakes firmly wedged between them. The upper piece of clear Scotch™ tape was then peeled back in order to pull apart the sheets composing the biotite flakes, and this piece of clear Scotch™ tape with thin biotite sheets adhering to it was then placed over a standard glass microscope slide, so that the adhesive side which had the thin mica flakes adhered to it became stuck onto the microscope slide. This procedure was repeated with another piece of clear Scotch™ tape placed over the original Scotch™ tape and biotite flakes affixed to the bench, the adhering biotite flakes being progressively pulled apart and transferred to microscope slides. As necessary, further hand-picked biotite flakes were added to replace those fully pulled apart. In this way tens of microscope slides were prepared for each sample, each with many (at least 20–30) thin biotite flakes mounted in them. This is similar to the method pioneered by Gentry. A minimum of 30 (usually 50) microscope slides was prepared for each sample to ensure good representative sampling statistics. Thus there was a minimum of 1,000 biotite flakes mounted on microscope slides for each sample.

Each thin section for each sample was then carefully examined under a petrological microscope in plane polarized light and all radiohalos present were identified, noting any relationships between the different radiohalo types and any unusual features. The numbers of each type of radiohalo in each slide were counted

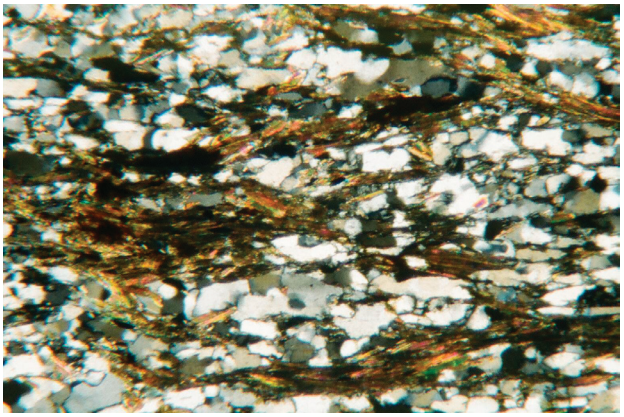

(a)

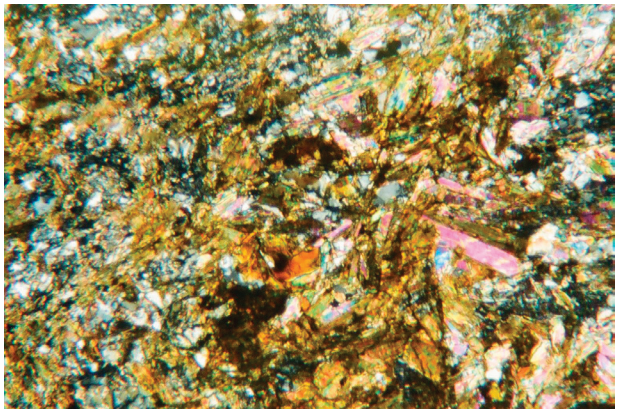

(b)

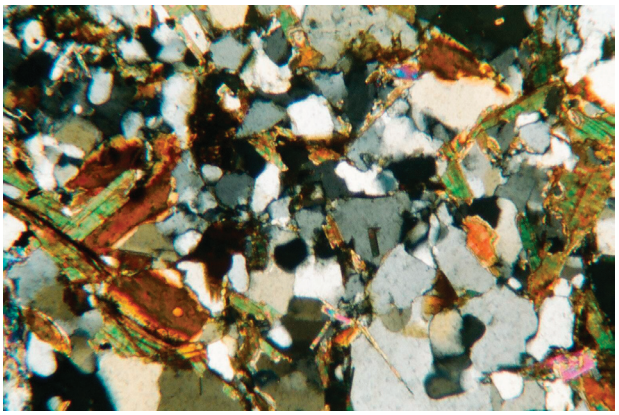

(c)

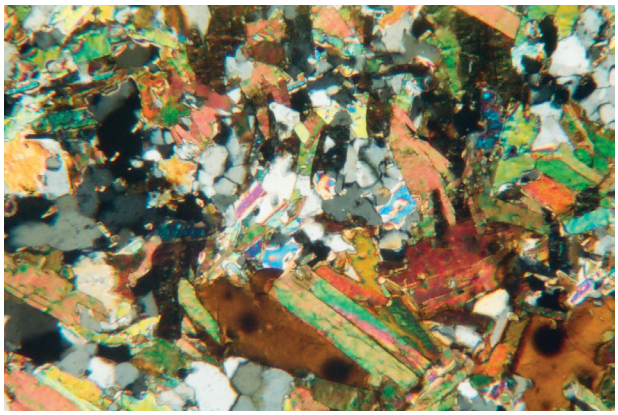

(d)

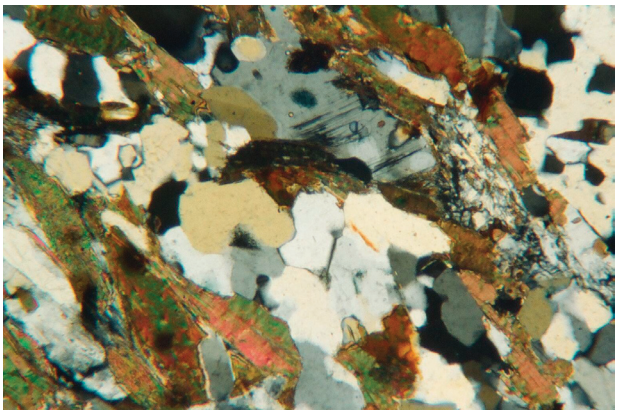

(e)

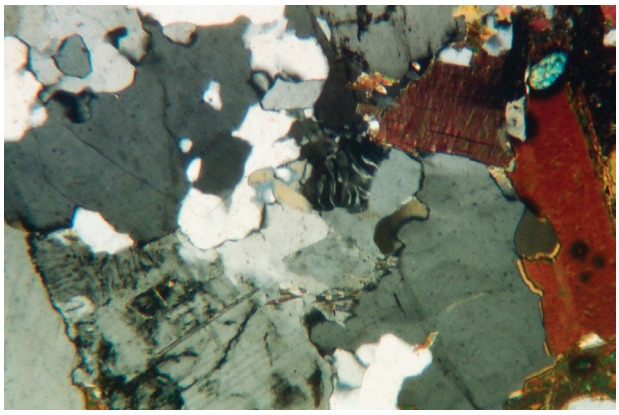

(f)

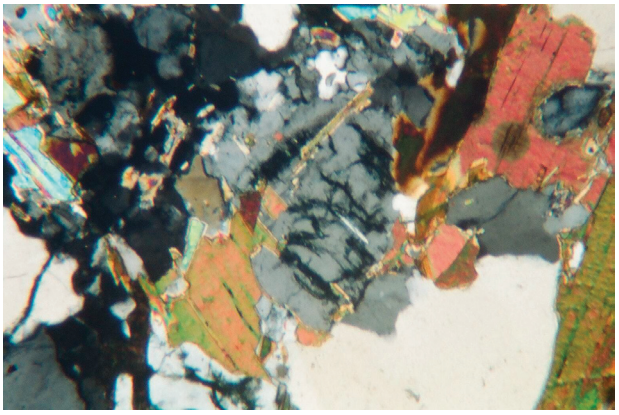

(g)

Fig. 4 (opposite). Representative photo-micrographs of the schists, gneisses, and granodiorite samples of the Cooma metamorphic complex, collected from the outcrops plotted on Fig. 2. All photo-micrographs are at the same scale (20× or 1 mm = 40 μm) and the rocks are as viewed under crossed polars.
(a) RMC-3 biotite zone schist: quartz, biotite, muscovite
(b) RMC-4 andalusite zone schist: quartz, biotite (with halos), muscovite
(c) RMC-5 K-feldspar zone gneiss: quartz, K-feldspar, biotite (with halos), muscovite
(d) RMC-6 K-feldspar zone gneiss: quartz, K-feldspar, biotite (with halos), muscovite
(e) RMC-7 migmatite zone gneiss: quartz, plagioclase, K-feldspar, biotite (with halos) muscovite
(f) RLG-2 Cooma granodiorite: quartz, plagioclase, K-feldspar, biotite (with halos), zircon
(g) RGC-1 Cooma granodiorite: quartz, plagioclase, K-feldspar, biotite (with halos), zircon, muscovite

by progressively moving the slide backwards and forwards across the field of view, and the numbers recorded for each slide were then tallied and tabulated for each sample. Only radiohalos whose radiocenters were clearly visible were counted. Because of the progressive peeling apart of many of the same biotite flakes during the preparation of the microscope slides, many of the radiohalos appeared on more than one microscope slide, so this procedure ensured each radiohalo was only counted once.

Results

Fig. 4 provides representative photomicrographs of the samples of schists and gneisses from the Cooma regional metamorphic complex. All radiohalos results are listed in Table 1. As predicted, all samples of the low-grade schists, high-grade gneisses and the granodiorite, except one of the two samples from the low-grade biotite zone, contained Po radiohalos. However, the two samples each from the biotite and andalusite zones only contained Po radiohalos, and almost exclusively ^{210}Po radiohalos. ^{238}U radiohalos were only present in the samples of the K-feldspar and migmatite zones, and the granodiorite, confirming the observations of Williams,[90] and ^{218}Po and ^{214}Po radiohalos were almost exclusively only found in those same samples. Some representative examples of the observed radiohalos can be seen in Fig. 5.

As well as the absolute numbers of each radiohalo type counted in each sample, Table 1 also shows the average total numbers of radiohalos per slide, and Po radiohalos per slide, plus abundance ratios for some pairs of radiohalo types. The total numbers of radiohalos and Po radiohalos per slide in the two biotite zone (low grade) samples averaged <1, but were numerous at an average of 11–12 per slide in the two andalusite zone samples. The highest average total numbers of radiohalos and Po radiohalos (~26 and 18–19 respectively) were in both the K-feldspar zone and the granodiorite samples (two each), more than double the average total number in the two andalusite zone samples. In stark contrast to this, the total number of radiohalos and Po radiohalos per slide, at 6 and 5 respectively, were significantly lower in the one migmatite zone sample.

Fig. 6 is a plot of the numbers of radiohalos per slide for each sample (vertical axis) along the west-east traverse across the regional metamorphic complex into the granodiorite (horizontal axis), as shown in Fig. 2. Four trends in the data are immediately evident. First, there is a rapid rise in the numbers of Po radiohalos with increasing metamorphic grade, from the biotite zone (low grade) through to the K-feldspar zone (high grade). Second, only

Table 1. Data table of radiohalos numbers counted in samples from the Cooma metamorphic complex and Cooma granodiorite.

Sample	Rock type	Slides	Radiohalos					Total Number of Radiohalos per Slide	Number of Po Radiohalos per Slide	Ratios	
			^{210}Po	^{214}Po	^{218}Po	^{238}U	^{232}Th			^{210}Po:^{238}U	^{210}Po:^{214}Po
RMC-1	Biotite zone schist	50	0	0	0	0	0	0	0	—	—
RMC-3	Biotite zone schist	50	63	0	0	0	0	1.26	1.26	—	—
RMC-2	Andalusite zone schist	50	592	0	0	0	0	11.84	11.84	—	—
RMC-4	Andalusite zone schist	50	557	2	0	0	0	11.18	11.18	—	278.5:1
RMC-5	K-feldspar zone schist	50	880	14	1	402	0	25.94	17.9	2.2:1	62.9:1
RMC-6	K-feldspar zone schist	50	1036	47	0	278	0	27.22	21.66	3.7:1	22:1
RMC-7	Migmatite	50	240	13	0	47	0	6.0	5.06	5.1:1	18.5:1
RLG-2	Granodiorite	41	373	44	0	418	37	21.27	10.17	0.9:1	8.5:1
RGC-1	Granodiorite	50	1175	0	81	318	0	31.48	25.12	3.7:1	—

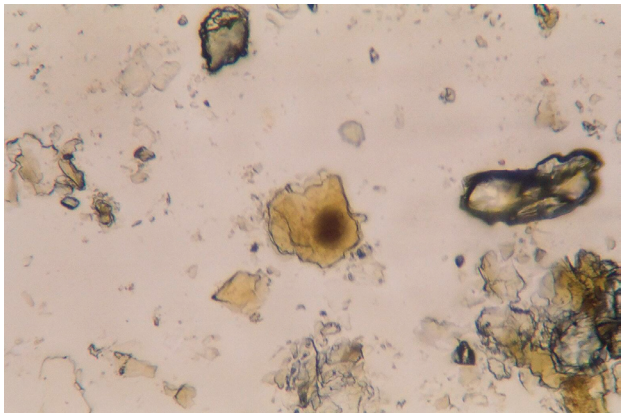

(a)

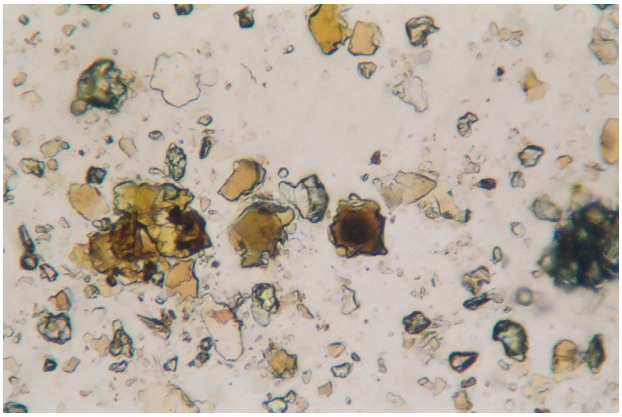

(b)

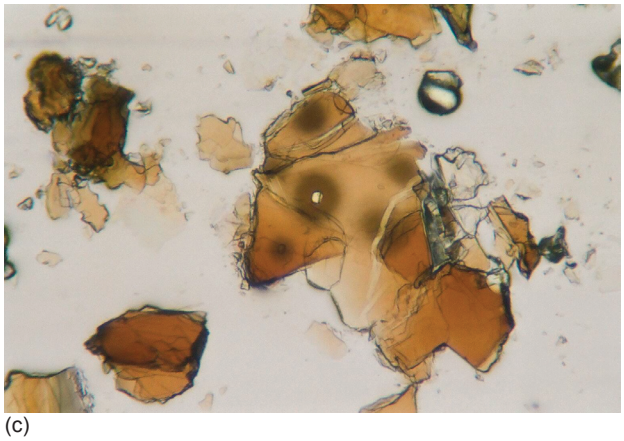

(c)

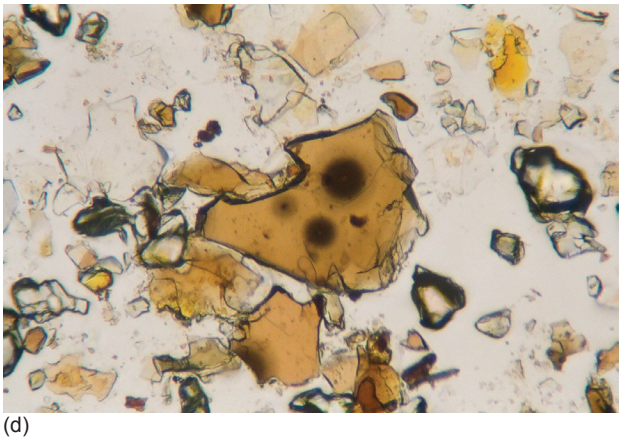

(d)

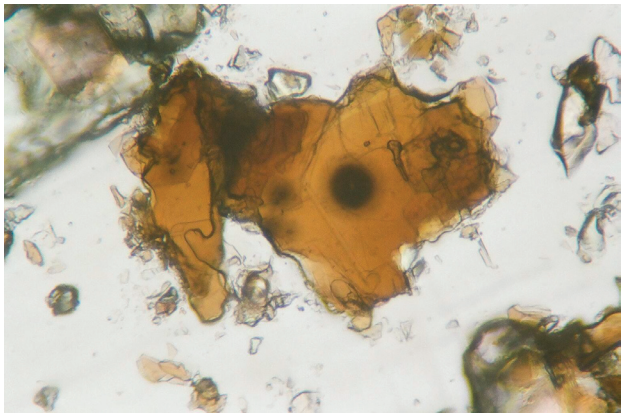

(e)

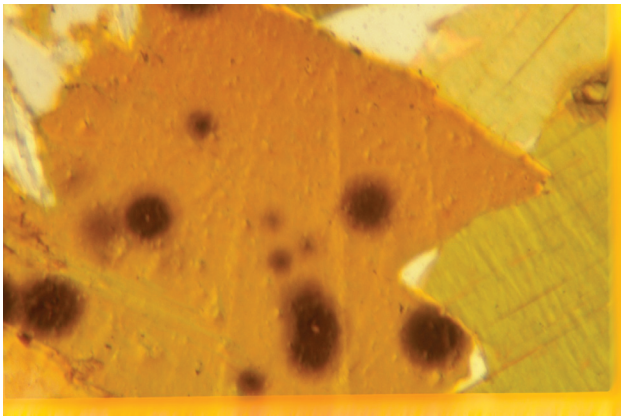

(f)

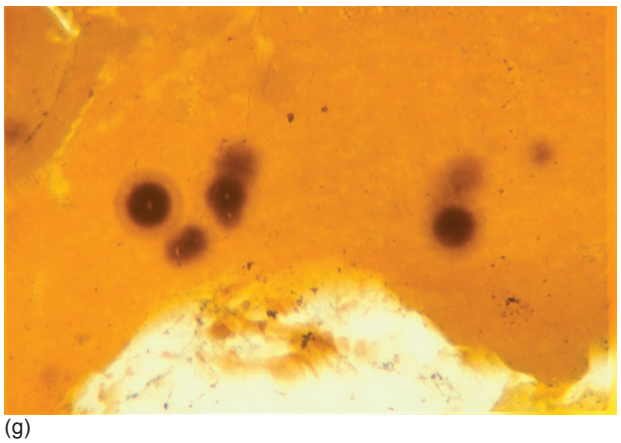

(g)

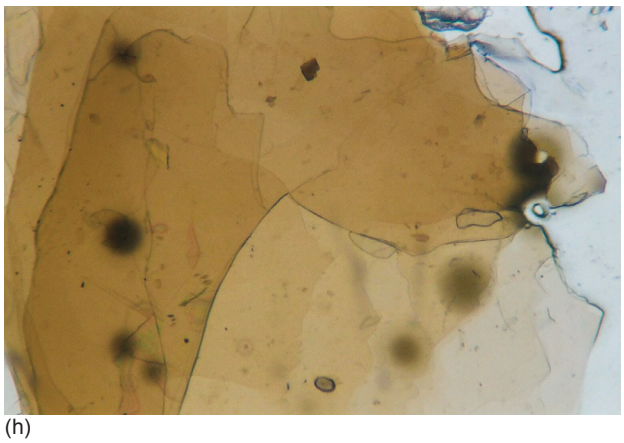

(h)

Fig. 5 (opposite). Some representative examples of radiohalos found in biotite grains separated from the schists and gneisses of the Cooma metamorphic complex and the Cooma granodiorite. All photo-micrographs are at the same scale (40× or 1 mm = 20 μm) and the biotite grains are as viewed in plane polarized light.
(a) RMC-3 biotite zone schist: two overlapping ^{210}Po radiohalos
(b) RMC-4 andalusite zone schist: a ^{210}Po radiohalo
(c) RMC-5 K-feldspar zone gneiss: two overexposed ^{238}U radiohalos and a ^{210}Po radiohalo
(d) RMC-6 K-feldspar zone gneiss: single ^{210}Po, ^{214}Po and an overexposed ^{238}U radiohalo
(e) RMC-7 migmatite zone gneiss: an overexposed ^{238}U and a ^{210}Po radiohalo
(f) RLG-2 Cooma granodiorite: four overexposed ^{238}U and five ^{210}Po radiohalos
(g) RLG-2 Cooma granodiorite: three overexposed ^{238}U and three ^{210}Po radiohalos
(h) RGC-1 Cooma granodiorite: two overexposed ^{238}U and four ^{210}Po radiohalos

the high grade zones (K-feldspar and migmatite) and the granodiorite have ^{238}U radiohalos in them. Third, the average total numbers of radiohalos and Po radiohalos in the high-grade K-feldspar zone and the granodiorite are both high and approximately the same. And fourth, there is a dramatic drop in the total numbers of both radiohalos and Po radiohalos in the migmatite zone.

Discussion

The significance of so many observed Po radiohalos in these Cooma metamorphic complex and Cooma granodiorite samples depends on how they are understood to have formed. In conventional thinking they are "a very tiny mystery" (G. Brent Dalrymple, as quoted by Gentry[91]) that can therefore be conveniently ignored because they have little apparent significance. However, if the formation of these Po radiohalos cannot be explained, then their significance cannot be fully comprehended. The reality is that the mystery of the Po radiohalos is ignored, because it constitutes a profound challenge to conventional wisdom.

Comprehensive reviews of what these Po radiohalos are and how they may have formed are provided by Gentry[92–95] and Snelling.[96] It has been established that all the observed Po radiohalos are generated exclusively from the Po radioisotopes in the ^{238}U decay series, namely, ^{218}Po, ^{214}Po, and ^{210}Po, with contributions from none of the other species in the ^{238}U α-decay chain (Gentry[97]). Furthermore, it has been estimated that, like the ^{238}U radiohalos, each visible Po radiohalo requires between 500 million and 1 billion α-decays to generate it (Gentry[98]), which equates to a corresponding number of Po atoms having been in each radiocenter. Thus the crucial issue is how did so many Po atoms get concentrated into these radiocenters to generate the Po radiohalos, when their half-lives are only 3.1 minutes (^{218}Po), 164 microseconds (^{214}Po), and 138 days (^{210}Po)?

Gentry[99–101] insists that the Po must be primordial, that is, created by God instantaneously in place in the radiocenters in the biotite flakes in the granites, and thus the granites are also created rocks. In other words, he argues that granites did not form from the crystallization and cooling of magmas, but rather are the earth's created foundation rocks. Moreover, where granites such as the Cooma granodiorite have been intruded into fossiliferous Flood-deposited strata, Gentry[102] insists that these granites also represent originally created rocks. He argues that during the Flood they were tectonically intruded as cold bodies, and that the contact metamorphic aureoles were produced by the heat and pressure generated during tectonic emplacement, augmented in some cases by hot fluids from depth.

Such an interpretation is inconsistent with the field and petrological evidence from the Cooma metamorphic complex and the Cooma granodiorite. The granodiorite is in fact the product of the regional metamorphism of the fossiliferous (Flood-deposited) sedimentary rocks that host the granodiorite, with a gradational boundary of migmatites (consisting of partially melted sediments). There is no fracturing, brecciation or mylonization that should be evident in either the granodiorite or these immediately adjacent metamorphic rocks if the granodiorite had been intruded tectonically as a cold body. Indeed, the biotite flakes in the metamorphic schists and gneisses that host the Po radiohalos were not in the original fossiliferous sediments, but are the product of the regional metamorphism of the sediments which post-dated their deposition. Therefore, the Po radiohalos must have formed after the biotite flakes formed, during the regional metamorphism and the generation of the granodiorite.

The four trends in the data (table 1 and fig. 6) are assumed here to be both real and significant, and thus require an attempted explanation. It was predicted that Po radiohalos would be found in these regionally metamorphosed pelitic and psammitic sediments because:
(1) The hydrothermal fluid transport model for Po radiohalo formation[103, 104] only requires biotite flakes which enclose tiny zircon grains containing ^{238}U, and hydrothermal fluids to flow along the biotite cleavage planes past the zircon grains;
(2) The schists and gneisses in the Cooma metamorphic complex contain both biotite flakes and zircon grains from the biotite zone schists inwards to the migmatite zone gneisses;[105, 106] and

(3) A proposed creationist model for regional metamorphism[107, 108] postulates hydrothermal fluids flowing through sediments are responsible for their regional metamorphism.

Of course, this prediction was also confidently made because:

(4) ^{238}U radiohalos had already been observed in the high grade gneisses of the Cooma metamorphic complex,[109] and reported in the Cooma granodiorite[110] along with Po radiohalos;[111] and

(5) Po radiohalos had already been observed in metamorphic rocks elsewhere.[112–114]

The increasing numbers of Po radiohalos in the schists and gneisses with increasing metamorphic grade (the first trend in fig. 5) would definitely not have been due to the increasing temperatures and pressures. It has been determined from the relevant experimental and calculated phase equilibria[115–117] that to have produced the migmatites containing cordierite would have required temperatures of approximately 700°C at pressures of 3.5–4.0 kbar.[118, 119] However, radiohalos in biotite are annealed at and above 150°C,[120] so all the currently observed radiohalos in both the schists and gneisses, and the granodiorite, had to form below that temperature. Thus this trend has to have been due to another factor.

Other evidence elsewhere[121–123] would suggest that the numbers of Po radiohalos generated are primarily related to the volume and flow of hydrothermal fluids, such that more hydrothermal fluid flow produces more Po radiohalos. Of course, this assumes that there are sufficient zircon grains to supply enough Po isotopes from ^{238}U decay, and biotite flakes to host the Po radiocenters and resultant Po radiohalos. Indeed, this relationship is a direct outworking of the hydrothermal fluid transport model for Po radiohalo formation.[124] Thus, greater numbers of Po radiohalos have been reported in granites responsible for, and hosting, hydrothermal metallic ore veins—for example, the Land's End Granite, Cornwall.[125] Furthermore, where hydrothermal fluids had been produced by mineral reactions at a specific pressure-temperature boundary between zones during regional metamorphism of a sequence of sandstones, four-five times more Po radiohalos were generated at that specific metamorphic boundary than elsewhere in that regional metamorphic complex, regardless of increasing metamorphic grade.[126, 127] In another example, where hydrothermal fluids flowing in narrow shear zones had rapidly metamorphosed the high-grade granulite wall rocks, Po radiohalos are now present in the resultant eclogite, a high-grade metamorphic rock that otherwise doesn't host Po radiohalos.[128] And then, in a sequentially intruded suite of nested granite plutons, where the hydrothermal fluid content of the granites correspondingly increased so that the last intruded central pluton was connected to coeval explosive, steam-driven volcanism, the numbers of Po radiohalos generated increased inwards within the nested suite of granite plutons.[129] These evidences not only support the hydrothermal fluid transport model for Po radiohalo formation, but explain this first trend in the Cooma Po radiohalos data, as due to more hydrothermal fluids flowing through the metamorphic complex with increasing metamorphic grade producing more Po radiohalos.

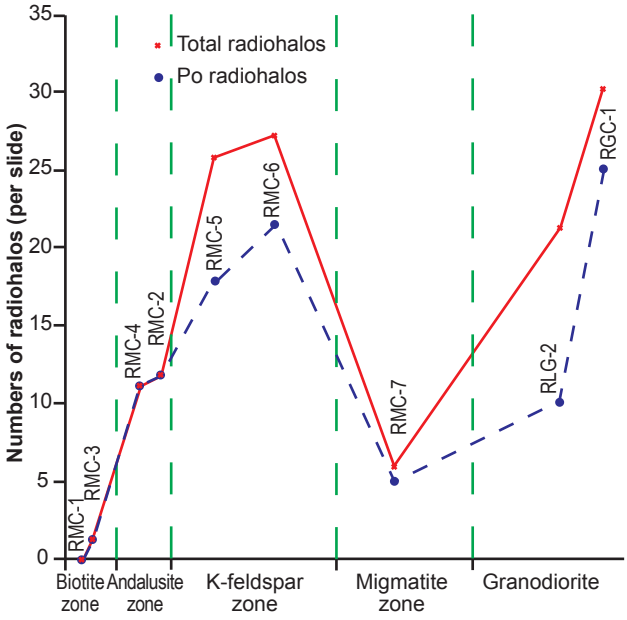

Fig. 6. Plot of numbers of radiohalos per slide in each sample along the west-east traverse shown in Fig. 2. The different metamorphic zones and the granodiorites are marked along the horizontal axis, and the relative lateral distances between sample locations are approximately to scale.

So why do only the high-grade K-feldspar and migmatite zones and the granodiorite have ^{238}U radiohalos in them (the second trend Fig. 6), when the low-grade biotite and andalusite zone schists also contain both zircon grains and biotite flakes? It can't be due to the ^{238}U radiohalos being annealed in the low-grade schists because of the elevated temperatures in them, because their Po radiohalos would also have been annealed. Besides, the temperatures in the high-grade gneisses and granodiorite were presumably even higher, yet both their Po and ^{238}U radiohalos have survived because of all being generated below 150°C. Furthermore, it can't be due to the zircons in the low-grade schists not having had ^{238}U in them, because they have been "flushed" by hydrothermal fluids of the Po derived by ^{238}U decay in them to generate the Po radiohalos in the schists' biotites, and the zircons in these schists have yielded U-Pb ages.[130] That potentially leaves only one likely explanation, namely, the zircon grains within the low-grade schists are not included in the biotite flakes. Obviously, to have ^{238}U radiohalos form around them, the tiny zircon grains

need to have been included in much larger biotite flakes, and that is the case in the high-grade gneisses and granodiorite. Neither Hopwood[131] nor Johnson, Vernon, and Hobbs[132] reported zircon grains being observed in the biotite zone schists, although Williams[133] reported some, albeit, as grains separated from the schists, rather than being observed within biotite flakes. On the other hand, Johnson, Vernon, and Hobbs reported zircon as an accessory mineral in the andalusite zone schists, and Williams separated zircon grains from them, so again the zircon grains may not have been in the schist's biotite flakes. The biotite flakes in the biotite zone schists can be as long as 0.7 mm,[134] potentially large enough to include zircon grains only 1–2 microns wide. However, the zircon grains separated from these low-grade schists by Williams are 75–150 microns long, too large to have ^{238}U radiohalos form around them, but still capable of supplying Po isotopes to passing hydrothermal fluids to generate Po radiocenters and radiohalos in the biotite flakes, even if the zircon grains were not enclosed in them.

Next is the third trend, namely, the numbers of ^{238}U and Po radiohalos are large, the same, and the highest both in the high-grade K-feldspar zone gneisses and the granodiorite (table 1 and fig. 6). If the major factor influencing the numbers of Po radiohalos generated is the volume of hydrothermal fluids in these rocks, then obviously the high grade zones and the granodiorite must have experienced the same greatest hydrothermal fluid flows within the complex. It must be remembered that because of the annealing of all radiohalos at and above 150 °C, these presently observed ^{238}U and Po radiohalos could only have formed after the regional metamorphism and after the granodiorite formed, as both the central granodiorite and the surrounding regional metamorphic complex together cooled below 150 °C. The general consensus is that the regional metamorphism occurred first, with the granodiorite an integral part of that event, but forming late in the development of the complex[135, 136] by virtually in situ partial melting of the high-grade metapsammites and migmatites.[137–147] Thus, if the granodiorite formation, crystallization, and cooling were the last to occur, then it was this that produced the last flux of hydrothermal fluids as the granodiorite and the surrounding metamorphic complex finally cooled below 150 °C. Because the granodiorite is central, then the hydrothermal fluids it produced when crystallizing and cooling flowed through it and then out from it. Thus the major impact of these hydrothermal fluids to generate Po radiohalos would have been in the granodiorite and in the surrounding high-grade gneisses, their effect rapidly waning with distance out to the low-grade zones as their passage slowed and temperatures fell.

Williams[148] also noted that in the low-grade biotite and andalusite zone schists the zircon grains are rounded and are thus totally detrital. On the other hand, in the high-grade K-feldspar and migmatite zone gneisses, and the granodiorite, there has been progressively more metamorphic and magmatic growth of the new zircon crystal faces over the original detrital zircon grains with increasing temperatures in the migmatite and granodiorite, and even the crystallization of new zircon grains. He concluded that below the K-feldspar isograd metamorphic conditions, zircon remained inert. However, at, or just before, the point of incipient partial melting, new zircon began to grow, implying some zircon had been dissolved in the partial melts. Because peraluminous melts and magmas, such as the Cooma migmatite leucosomes and the granodiorite, become zircon-saturated at relatively low Zr contents,[149] and zircon crystallization and new growth is controlled mainly by the degree of zircon supersaturation of the melt,[150] it was likely inevitable that some new zircon crystals grew. This may perhaps have been another factor in why there are ^{238}U radiohalos only in the high-grade K-feldspar and migmatite zone gneisses and the granodiorite.

Given these considerations, why then is there a dramatic drop in the numbers of both ^{238}U and Po radiohalos in the high-grade migmatite zone gneisses, the fourth trend noted in Table 1 and Fig. 6? If the generation of Po radiohalos is dependent on hydrothermal fluid flow, and the greater the fluid volume the more Po radiohalos are generated, then it follows that in the migmatite zone there must have been another factor operating to reduce the hydrothermal fluid flows, and/or their effectiveness in generating Po radiohalos. It has already been concluded above that the major impact of the hydrothermal fluids, produced by this last-stage granodiorite crystallizing and cooling to generate Po radiohalos as the whole complex cooled, would have been in the granodiorite and in the surrounding high-grade gneisses. That major impact is observed in the greatest numbers of Po radiohalos in the granodiorite and in the K-feldspar zone gneisses, but not in the migmatite zone gneisses.

This apparent enigma is resolved when the conditions under which partial melting occur are understood. It has long been known experimentally that apart from temperature and pressure, the major factor involved in partial melting is the presence and availability of water.[151] The temperatures required for partial melting are significantly lowered by increasing water activity up to saturation, and the amount of temperature lowering increases with increasing pressure.[152] At the temperatures of 650–700 °C and pressures of 3.5–4.0 kbar required to produce the Cooma migmatites containing cordierite,[153] the partial melting involved would have been under conditions of water saturation (Flood & Vernon, 1978). Furthermore, the water aids the partial melting process by dissolving in the melt, the water solubility in granitic melts increasing with pressure (and thus depth), so whereas at 1 kbar (equivalent to 3–4 km depth) the water solubility is 3.7 wt%,[154] at 30 kbar (up to 100 km depth)

it is approximately 24 wt%.[155] Thus the partial melting in the migmatite zone would have, in effect, largely used up whatever water was available in the rocks, and the water dissolved in the melt, when the latter crystallized, would have partitioned into mineral lattices, such as the biotite in selvedges around some leucosomes. There would, therefore, have been less hydrothermal fluids available during the cooling of the migmatite zone to generate Po radiohalos.

Three of the four trends in the radiohalo abundance data (table 1 and fig. 6), therefore, appear to be primarily related to the availability and volume of the hydrothermal fluids that were released from the central granodiorite after crystallization as it cooled to below 150°C, and then flowed out from the granodiorite into the surrounding metamorphic complex. Thus the presently observed Po radiohalos in the metamorphic complex appear to be a consequence of the intrusion, crystallization, and cooling of the granodiorite, rather than due to the processes that formed the regional metamorphic complex. Indeed, as previously discussed, the general consensus is that the formation of the granodiorite by in situ partial melting was a consequence of the regional metamorphism and not its cause. This is supported by the isotopic uniqueness of this granodiorite compared to the many other granitic rocks in the Lachlan Fold Belt—the highest initial $^{87}Sr/^{86}Sr$ values (0.7195), the greatest negative initial Nd values (ε_{Nd}=–9.2), and the highest $\delta^{18}O$ values (12.9)[156–158]—all suggestive of a different origin for this granodiorite compared to the many other granitic rocks in the Lachlan Fold Belt.

Therefore, it has been suggested that the heat which caused the regional metamorphism was probably introduced to the lower crust of this region by large-scale mantle processes due to a major shift in the patterns of asthenospheric (upper mantle) convection.[159] Such large-scale mantle processes are also credited with the initiation of the large-scale lower crustal partial melting to generate the tens to hundreds of granitic plutons in regional batholiths, so it has also been suggested that the Cooma regional metamorphism was related to emplacement of the adjacent Murrumbidgee Batholith.[160] Indeed, Richards and Collins[161] provide evidence to support their claim that the Cooma complex represents a regional metamorphic aureole developed around the Murrumbidgee Batholith.

Snelling[162, 163] has reviewed the mounting evidence in conventional thinking that granite magma generation, intrusion, crystallization, and cooling are rapid dynamic processes requiring only tens to hundreds of years within a uniformitarian time framework, compared to the 100,000 to 1 million years originally claimed. Conventional plate tectonics at uniformitarian slow rates is postulated to be responsible for the large-scale upper mantle convection that delivered heat to partially melt the lower crust and thereby generate granite batholiths. However, in the context of the Flood event in the biblical framework for earth history, these processes are postulated to have occurred at catastrophic rates during catastrophic plate tectonics.[164] The catastrophic large-scale generation of a granite batholith, such as the Murrumbidgee Batholith in the Lachlan Fold Belt, would have resulted in the many constituent intruded plutons all emanating heat with the released convecting hydrothermal fluids as they crystallized and cooled, thus producing a regional metamorphic aureole around the batholith. This is consistent with a catastrophic model for regional metamorphism in which the heat and hydrothermal fluids acting on the mineral constituents of the original sediment layers rapidly produced the regional metamorphic zones with their index minerals designating the different metamorphic grades, as in the Cooma complex.[165] Based on the catastrophic rate for granite formation of 6–10 days,[166, 167] this regional metamorphic complex would thus have been produced during this same timescale of 6–10 days over which the granite batholith was emplaced and cooled.

However, this regional metamorphic event reached its climax within that 6–10 days timescale with the partial melting that generated the Cooma granodiorite, which is thus, in effect, a secondary product of the emplacement of the Murrumbidgee Batholith. According to Flood and Vernon,[168] the large-scale partial melting at depth to produce the Cooma granodiorite as a consequence of the generation of this regional metamorphic aureole would have resulted in the melt segregating and being emplaced within the center of the regional metamorphic complex, attenuating the metamorphic zoning to leave the asymmetric zonal pattern observed today. The further 6–10 days timescale for the formation and cooling of the secondary Cooma granodiorite[169,170] would have commenced within the 6–10 days timescale for the formation of the granite batholith, so the total timescale for the formation of this regional metamorphic complex with its central granodiorite would have been on the order of 12–20 days. This is consistent with the Po radiohalos produced by the hydrothermal fluids released by the cooling central granodiorite in the latter part of this period, because the ^{214}Po and ^{210}Po radiohalos in the schists and gneisses would have formed within hours and days respectively,[171] after the granodiorite and the metamorphic complex both cooled below 150°C.

It might be argued that alternately the temperature fall in both the granite and the metamorphic complex could have been gradual over thousand of years, and when the temperature reached 150°C the continued outflow of hydrothermal fluids at lower temperatures over further decades provided the necessary conditions for Po

radiohalo generation in different loci at different times. However, Snelling[172] has shown that the Po radiohalos in granites could only have been generated within hours to a few days concurrently while the ^{238}U radiohalos were also forming, and while the ^{238}U decay in their zircon radiocenters to provide the necessary Po (before it decayed) was grossly accelerated. Furthermore, Snelling[173] has argued that below 150°C the hydrothermal fluid flows cannot be long sustained, because most of the heat energy to drive the needed convection system[174] that both cools the granite and transports the Po has already been dissipated while the temperature in the granite rapidly falls from 400°C to 150°C. Thus, these evidences combined are consistent with the emplacement and cooling of these granite plutons within 6–10 days.

Apparent U-Pb, Rb-Sr, Kr-Ar, and Ar-Ar ages of minerals from the Cooma granodiorite and metamorphic complex[175–177] can be used to construct a cooling history curve for the Cooma granodiorite and metamorphic complex,[178–181] based on the effective closure temperatures of those minerals. According to this curve, the granodiorite and metamorphic complex supposedly took 45 million years to cool from 735 to 150°C. However, if as has been shown from several lines of evidence, radioisotope decay rates were grossly accelerated during the Flood event,[182] while catastrophic plate tectonics were operating to produce catastrophic granite formation, then this cooling would have occurred within days, which is consistent with the timescales for granite formation[183,184] and Po radiohalos generation.[185]

Conclusions

The Cooma granodiorite was generated as a consequence of the regional metamorphism that resulted from the catastrophic large-scale emplacement of the Murrumbidgee Batholith during the catastrophic plate tectonics of the year-long Flood event. The Cooma metamorphic complex was generated as a regional aureole by the heat and hydrothermal fluids released by the batholith interacting with the mineral constituents of the original, fossil-bearing, Flood-deposited sediments it intruded within 6–10 days to produce the regional metamorphic zones. At the peak of this regional metamorphism, partial melting at depth at the center of the complex formed the granodiorite, which was then emplaced within the complex. As the granodiorite crystallized and cooled, the hydrothermal fluids emanating from it generated Po radiohalos within the granodiorite and within the surrounding metamorphic complex in hours to days as the terrain cooled below 150°C. This would have occurred towards the end of the further 6–10 days in which the granodiorite formed and cooled. Thus this regional metamorphic complex and its centrally-generated granodiorite with the contained Po radiohalos only took 12–20 days in total to form and cool. The observed patterns of Po radiohalos are consistent with the availability and volume of the hydrothermal fluids responsible for transporting the necessary Po isotopes from the source zircons in the granodiorite, gneisses and schists to form the Po radiocenters that generated the Po radiohalos. Thus, where there was a high volume of hydrothermal fluids in the granodiorite and the immediately surrounding gneisses of the high-grade zones, large numbers of Po radiohalos were generated, except in the migmatite zone where the water aided partial melting, was dissolved in the melt, and then was partitioned into minerals as they crystallized. Where the volume of hydrothermal fluids progressively diminished further out in the low-grade schists, the numbers of Po radiohalos rapidly diminished outwards through the andalusite and biotite zones. In conclusion, not only do the radiohalos in the Cooma metamorphic complex support the hydrothermal fluid transport model for Po radiohalos generation,[186] but they and their context are consistent with creationist models for catastrophic granite formation[187, 188] and catastrophic regional metamorphism[189] during the catastrophic plate tectonics[190] of the year-long biblical Flood.

Acknowledgments

This research would not have been achieved without the help and support of numerous people. First, there was the forbearance and support of my wife Kym and family in allowing the necessary field work and sampling during travel on family vacations. Second, Mark Armitage assisted with the processing of samples and the counting of radiohalos. Third, the Institute for Creation Research funded Mark's help and my time on this project. And finally, there was the constant patience and support of my wife and family, and the Lord's help overall and in pulling together the pieces of the puzzle.

References

1. Browne, W.R., 1914. The geology of the Cooma District, NSW, Part 1. *Journal and Proceedings of the Royal Society of New South Wales* **48**:172–222.
2. Johnson, S.E., R.H. Vernon, and B.E. Hobbs, 1994. *Deformation and metamorphism of the Cooma Complex, southeastern Australia.* Specialist group in tectonics and structural geology, Geological Society of Australia, Sydney, Field Guide No. 4.
3. Johnson et al., Ref. 2.

4. Joplin, G.A., 1942. Petrological studies in the Ordovician of New South Wales. I. The Cooma Complex. *Proceedings of the Linnean Society of New South Wales* **67**:156–196.
5. Joplin, G.A., 1962. An apparent magmatic cycle in the Tasman Geosyncline. *Journal of the Geological Society of Australia* **9**:51–69.
6. Joplin, Ref. 4.
7. Miyashiro, A., 1973. *Metamorphism and metamorphic belts*. London: George Allen and Unwin.
8. Hall, A., 1996,. *Igneous petrology*, 2nd ed. Harlow, England: Addison Wesley Longman.
9. Richards, S.W., W.J. Collins, and J. Needham, 2000. The Cooma Complex: A crustal scale magma transfer zone of the Murrumbidgee Batholith. *Geological Society of Australia Abstracts* **59**:417.
10. Joplin, Ref. 4.
11. Joplin, G.A., 1968. *A petrography of Australian metamorphic rocks*. Sydney: Angus and Robertson.
12. Hopwood, T.P., 1969. Southern and central highlands fold belt: Cooma district. In, Packham, G.H. (ed.), *The geology of New South Wales. Journal of the Geological Society of Australia* **16**:93–96.
13. Hopwood, T.P., 1976. Stratigraphy and structural summary of the Cooma Metamorphic Complex. *Journal of the Geological Society of Australia* **23**:345–360.
14. Chappell, B.W. and A.J.R. White, 1976. Cooma Granodiorite and associated metamorphic rocks. In *Plutonic rocks of the Lachlan mobile zone*, pp. 17–19. Sydney: 25th International Geological Congress Field Guide 13C.
15. Chappell, B.W., A.J.R. White, and I.S. Williams, 1991. A transverse section through granites of the Lachlan Fold Belt. *Second Hutton Symposium on granites and related rocks*. Australian Bureau of Mineral Resources, Record 1991/22.
16. Johnson et al., Ref. 2.
17. Johnson, S.E., 1992. Sequential porphyroblast growth during progressive deformation and low-P high-T (LPHT) metamorphism, Cooma Complex, Australia: The use of microstructural analysis to better understand deformation and metamorphic histories. *Tectonophysics* **214**:311–339.
18. Johnson et al., Ref. 2.
19. Johnson, Ref. 17.
20. Johnson, S.E., 1999. Deformation and possible origins of the Cooma Complex, southeastern Lachlan Fold Belt, New South Wales. *Australian Journal of Earth Sciences* **46**:429–442.
21. Hopwood, Ref. 12.
22. Hopwood, Ref. 13.
23. Hopwood, Ref. 12.
24. Fergusson, C.L. and C.M. Fanning, 2002. Late Ordovician stratigraphy, zircon provenance and tectonics, Lachlan Fold Belt, Southeastern Australia. *Australian Journal of Earth Sciences* **49**:423–436.
25. Sherrard, K.M., 1954. The assemblages of graptolites in New South Wales. *Journal and Proceedings of the Royal Society of New South Wales* **87**:73–101.
26. Williams, I.S., 2001. Response of detrital zircon and monazite, and their U-Pb isotopic systems, to regional metamorphism and host-rock partial melting, Cooma Complex, southwestern Australia. *Australian Journal of Earth Sciences* **48**:557–580.
27. Fergusson and Fanning, Ref. 24.
28. Johnson, S.E. and R.H. Vernon, 1995. Stepping stones and pitfalls in the determination of an anticlockwise P-T-t deformation path: The low-P high-T Cooma Complex, Australia. *Journal of Metamorphic Geology* **13**:165–183.
29. Richards, S.W., and W.J. Collins, 2002. The Cooma metamorphic complex, a low-P, high-T (LPHT) regional aureole beneath the Murrumbidgee Batholith. *Journal of Metamorphic Geology* **20**:119–134.
30. Miyashiro, A., 1958. Regional geology of the Gosaisya-Takanuki district in the Central Abukuma Plateau. *Journal of the Faculty of Science University of Tokyo* **11**:219–272.
31. Chappell et al., Ref. 15.
32. Hopwood, Ref. 13.
33. Johnson et al., Ref. 2.
34. Hopwood, Ref. 13.
35. Johnson et al., Ref. 2.
36. Johnson et al., Ref. 2.
37. Hopwood, Ref. 13.
38. Johnson et al., Ref. 2.
39. Chappell et al., Ref. 15.
40. Munksgaard, N.C., 1988. Source of the Cooma Granodiorite, New South Wales—a possible role of fluid-rock interactions. *Australian Journal of Earth Sciences* **35**:498–512.
41. Ellis, D.J., and M. Obata, 1992. Migmatite and melt segregation at Cooma, New South Wales. *Transactions of the Royal Society of Edinburgh: Earth Sciences* **83**:95–106.
42. Johnson et al., Ref. 2.
43. Williams, Ref. 26.
44. Snelling, A.A. and M.H. Armitage, 2003. Radiohalos—a tale of three granitic plutons. In, Ivey, R.L. Jr. (ed.), *Proceedings of the fifth international conference on creationism*, pp. 243–267. Pittsburgh, Pennsylvania: Creation Science Fellowship.
45. Snelling, A.A., 2005a. Radiohalos in granites: Evidence for accelerated nuclear decay. In, Vardiman, L., A.A. Snelling, abd E.F. Chaffin (eds.), *Radioisotopes and the age of the earth: Results of a young-earth creationist research initiative*,

pp. 101–207. El Cajon, California: Institute for Creation Research and Chino Valley, Arizona: Creation Research Society.
46. Snelling, A.A., 2005b. Polonium radiohalos: The model for their formation tested and verified. *Impact #386*. El Cajon, California: Institute for Creation Research.
47. Snelling, A.A., 2008a. Testing the hydrothermal fluid transport model for polonium radiohalo formation: The Thunderhead Sandstone, Great Smoky Mountains, Tennessee-North Carolina. *Answers Research Journal* **1**:53–64.
48. Snelling, A.A., 1994a. Towards a creationist explanation of regional metamorphism. *Creation Ex Nihilo Technical Journal* **8**(1):51–77.
49. Snelling, Ref. 45.
50. Snelling and Armitage, Ref. 44.
51. Chappell and White, Ref. 14.
52. Ellis and Obata, Ref. 41.
53. Joplin, Ref. 4.
54. Williams Ref. 26.
55. Snelling and Armitage, Ref. 44.
56. Johnson et al., Ref. 2.
57. Chappell, B.W., and A.J.R. White, 1974. Two contrasting granite types. *Pacific Geology* **8**:173–274.
58. Chappell et al., Ref. 15.
59. Chappell et al., Ref. 15.
60. Chappell et al., Ref. 15.
61. McCulloch, M.T., and B.W. Chappell, 1982. Nd isotopic characteristics of S- and I-type granites. *Earth and Planetary Science Letters* **58**:51–64.
62. Munksgaard, Ref. 40.
63. Pidgeon, R.T., and W. Compston, 1965. The age and origin of the Cooma Granodiorite and its associated metamorphic zones, New South Wales. *Journal of Petrology* **6**:193–222.
64. Williams, Ref. 26.
65. White, A.J.R., B.W. Chappell, and J.R. Cleary, 1974. Geologic setting and emplacement of some Australian Palaeozoic batholiths and indications for intrusion mechanisms. *Pacific Geology* **8**:159–171.
66. Chappell and White, Ref. 14.
67. Chappell et al., Ref. 15.
68. Pidgeon and Compston, Ref. 63.
69. Munksgaard, Ref. 62.
70. Tetley, N., 1979. Geochronology and thermal history of the Cooma Granodiorite. *Australian Bureau of Mineral resources record*, 1979/2, pp. 88–89.
71. Chappell et al., Ref. 15.
72. Tetley, Ref. 70.
73. Williams, Ref. 26.
74. Wiliams, Ref. 26.
75. Chappell et al., Ref. 15.
76. Ellis and Obata, Ref. 41.
77. Gray, C.M., 1984. An isotopic mixing model for the origin of granitic rocks in southeast Australia. *Earth and Planetary Science Letters* **70**:47–60.
78. Joplin, Ref. 4.
79. Joplin, Ref. 5.
80. McCulloch and Chappell, Ref. 61.
81. Munksgaard, Ref. 62.
82. Pidgeon and Compson, Ref. 63.
83. White, A.J.R. and B.W. Chappell, 1988. Some supracrustal (S-type) granites of the Lachlan Fold Belt. *Transactions of the Royal Society of Edinburgh: Earth Science* **79**:169–181.
84. White et al., Ref. 65.
85. Flood, R.H., and R.H. Vernon, 1978. The Cooma Granodiorite, Australia: An example of in situ crustal anatexis? *Geology* **6**:81–84.
86. Troitzsch, U., 1995. *A petrological study of the high-grade metamorphic rocks of the Cooma Complex, New South Wales, Australia*. Unpublished diploma thesis. Darmstadt, Germany: Technische Hochschule Darmstadt.
87. Richards et al., Ref. 9.
88. Vernon, R.H., S.W. Richards, and B.F. Collins, 2001. Migmatite-granite relationships: origin of the Cooma Granodiorite magma, Lachlan Fold Belt, Australia. *Physics and Chemistry of the Earth (A)* **26**(4–5):267–271.
89. Williams, Ref. 26.
90. Williams, Ref. 26.
91. Gentry, R.V., 1988. *Creation's tiny mystery*, p. 122. Knoxville, Tennessee: Earth Science Associates.
92. Gentry, R.V., 1973. Radioactive halos. *Annual Review of Nuclear Science* **23**:347–362.
93. Gentry, R.V., 1974. Radiohalos in a radiochronological and cosmological perspective. *Science* **184**:62–66.
94. Gentry, R.V., 1984. Radioactive halos in a radiochronological and cosmological perspective. *Proceedings of the 63rd annual*

meeting, Pacific division, American Association for the Advancement of Science **1**(3):38–65.
95. Gentry, R.V., 1986. Radioactive haloes: Implications for creation. In, Walsh, R.E., C.L. Brooks, and R.S. Crowell (eds.), *Proceedings of the first international conference on creationism*, Vol. 2, pp. 89–112. Pittsburgh, Pennsylvania: Creation Science Fellowship.
96. Snelling, A.A., 2000. Radiohalos. In, Vardiman, L., A.A. Snelling, and E.F. Chaffin (eds.), *Radioisotopes and the age of the earth: A young-earth creationist research initiative*, pp. 381–468. El Cajon, California: Institute for Creation Research and St. Joseph, Missouri: Creation Research Society.
97. Gentry, Ref. 93.
98. Gentry, R.V., 1988. *Creation's tiny mystery.* Knoxville, Tennessee: Earth Science Associates.
99. Gentry, Ref. 95.
100. Gentry, Ref. 98.
101. Gentry, R.V., 1989. Response to Wise. *Creation Research Society Quarterly* **25**:176–180.
102. Gentry, Ref. 101.
103. Snelling, Ref. 45.
104. Snelling and Armitage, Ref. 44.
105. Johnson et al., Ref. 2.
106. Williams, Ref. 26.
107. Snelling, Ref. 48.
108. Snelling, A.A., 1994b. Regional metamorphism within a creationist framework: what garnet compositions reveal. In, Walsh, Walsh (ed.), *Proceedings of the third international conference on creationism*, pp. 485–496. Pittsburgh, Pennsylvania: Creation Science Fellowship.
109. Williams, Ref. 26.
110. Williams, Ref. 26.
111. Snelling and Armitage, Ref. 44.
112. Snelling, Ref. 45.
113. Snelling, Ref. 46.
114. Snelling, Ref. 47.
115. Powell, R., and T.J.B. Holland, 1990. Calculated mineral equilibria in the pelite system, KFMASH (K_2O-FeO-MgO-Al_2O_3-SiO_2-H_2O). *American Mineralogist* **75**:367–380.
116. Seifert, F., 1976. Stability of the assemblage cordierite+K feldspar+quartz. *Contributions to Mineralogy and Petrology* **57**: 179–185.
117. Spear, F.S., and J.T. Cheney, 1989. A petrogenetic grid for pelitic schists in the system SiO_2-Al_2O_3-FeO-MgO-K_2O-H_2O. *Contributions to Mineralogy and Petrology* **101**:149–164.
118. Ellis and Obata, Ref. 41.
119. Johnson and Vernon, Ref. 28.
120. Laney, R., and A.W. Laughlin, 1981. Natural annealing of the pleochroic haloes in biotite samples from deep drill holes, Fenton Hill, New Mexico. *Geophysical Research Letters* **8**(5):501–504.
121. Snelling, Ref. 46.
122. Snelling, A.A., 2006a. Confirmation of rapid metamorphism of rocks. *Impact #392.* El Cajon, California: Institute for Creation Research.
123. Snelling, Ref. 47.
124. Snelling, Ref. 45.
125. Snelling, Ref. 45.
126. Snelling, Ref. 46.
127. Snelling, Ref. 47.
128. Snelling, Ref. 122.
129. Snelling, A.A., and D. Gates, 2008. The implications of Po radiohalos in the nested plutons of the Tuolumne Intrusive Suite, Yosemite. *Answers Research Journal* **1**, in preparation.
130. Williams, Ref. 26.
131, Hopwood, Ref. 13.
132. Johnson et al., Ref. 2.
133. Williams, Ref. 26.
134. Johnson et al., Ref. 2.
135. Johnson, Ref. 17.
136. Johnson, Ref. 20.
137. Chappell et al., Ref. 15.
138. Ellis and Obata, Ref. 41.
139. Gray, Ref. 77.
140. Joplin, Ref. 4.
141. Joplin, Ref. 5.
142. McCulloch and Chappell, Ref. 61.
143. Munksgaard, Ref. 62.

144. Pidgeon and Compston, Ref. 63.
145. Vernon et al., Ref. 88.
146. White and Chappell, Ref. 83.
147. White et al., Ref. 65.
148. Williams, Ref. 26.
149. Watson, E.B. and T.M. Harrison, 1983. Zircon saturation revisited: temperature and composition effects in a variety of crustal magma types. *Earth and Planetary Science Letters* **64**:295–304.
150. Varva, G., 1990. On the kinematics of zircon growth and its petrogenetic significance: A cathodoluminescence study. *Contributions to Mineralogy and Petrology* **106**:90–99.
151. Tuttle, O.F. and N.L. Bowen, 1958. Origin of granite in the light of experimental studies in the system $NaAlSi_3O_8$-$KAlSi_3O_8$-SiO_2-H_2O. *Geological Society of America Memoir 71.*
152. Ebadi, A., and W. Johannes, 1991. Beginning of melting and composition of first melts in the system Qz-Ab-Or-H_2O-CO_2. *Contributions to Mineralogy and Petrology* **106**:286–295.
153. Ellis and Obata, Ref. 41.
154. Holtz, F., H. Behrens, D.B. Dingwell, and W. Johannes, 1995. Water solubility in haplogranitic melts: compositional, pressure and temperature dependence. *American Mineralogist* **80**:94–108.
155. Huang, W.L., and P.J. Wyllie, 1975. Melting reactions in the system $NaAlSi_3O_8$-$KAlSi_3O_8$-SiO_2 to 35 kilobars, dry with excess water. *Journal of Geology* **83**:737–748.
156. Gray, Ref. 77.
157. McCulloch and Chappell, Ref. 61.
158. Munksgaard, Ref. 62.
159. Williams, Ref. 26.
160. Richards, Collins and Needham, Ref. 9.
161. Richards and Collins, Ref. 29.
162. Snelling, A.A., 2006b. Catastrophic granite formation: Rapid melting of sedimentary and metamorphic rocks, and rapid magma intrusion and cooling. In, *Yosemite/Death Valley guidebook*, chap. 2, pp. 17–28. Santee, California: Institute for Creation Research.
163. Snelling, A.A., 2008b. Catastrophic granite formation: Rapid melting of source rocks, and rapid magma intrusion and cooling. *Answers Research Journal* **1**:11–25.
164. Austin, S.A., J.R. Baumgardner, D.R. Humphreys, A.A. Snelling, L. Vardiman, and K.P. Wise, 1994. Catastrophic plate tectonics: A global Flood model of earth history. In, Walsh, R.E. (ed.), *Proceedings of the third international conference on creationism*, pp. 609–621. Pittsburgh, Pennsylvania: Creation Science Fellowship.
165. Snelling, Ref. 48.
166. Snelling, Ref. 162.
167. Snelling, Ref. 163.
168. Flood and Vernon, Ref. 85.
169. Snelling, Ref. 162.
170. Snelling, Ref. 163.
171. Snelling, Ref. 45.
172. Snelling, Ref. 45.
173. Snelling, Ref. 163.
174. Snelling, A.A., and J. Woodmorappe, 1998. The cooling of thick igneous bodies on a young earth. In, Walsh, R.E. (ed.), *Proceedings of the fourth international conference on creationism*, pp. 527–545. Pittsburgh, Pennsylvania: Creation Science Fellowship.
175. Pidgeon and Compston, Ref. 63.
176. Tetley, Ref. 70.
177. Williams, Ref. 26.
178. Tetley, Ref. 70.
179. Chappell et al., Ref. 15.
180. Johnson et al., Ref. 2.
181. Williams, Ref. 26.
182. Vardiman, L., A.A. Snelling, and E.F. Chaffin (eds), 2005. *Radioisotopes and the age of the earth: Results of a young-earth creationist research initiative.* El Cajon, California: Institute for Creation Research and Chino Valley, Arizona: Creation Research Society.
183. Snelling, Ref. 162.
184. Snelling, Ref. 163.
185. Snelling, Ref. 46.
186. Snelling, Ref. 45.
187. Snelling, Ref. 162.
188. Snelling, Ref. 163.
189. Snelling, Ref. 108.
190. Austin et al., Ref. 164.